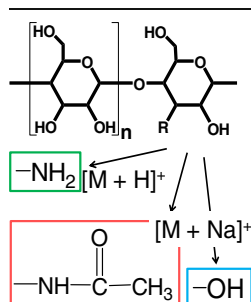


## RESEARCH ARTICLE

# Amino and Acetamide Functional Group Effects on the Ionization and Fragmentation of Sugar Chains in Positive-Ion Mass Spectrometry

Tohru Yamagaki, Kohtaro Sugahara, Takehiro Watanabe

Suntory Institute for Bioorganic Research, Mishima, Osaka 618-8503, Japan



**Abstract.** To elucidate the influence of amino ( $-\text{NH}_2$ ) and acetamide ( $-\text{NHCOCH}_3$ , -NAC) groups in sugar chains on their ionization and fragmentation, cyclodextrins (cyclodextrins, CyDs) and lacto-oligosaccharide are analyzed by MALDI TOF/TOF and ESI Q-TOF mass spectrometry. CyD derivatives substituted by amino or acetamide groups are ideal analytes to extract the function group effects, which are amino-CyD with one hexosamine (HexNH<sub>2</sub>) and acetamide-CyD with one *N*-acetyl hexosamine (HexNAC). Interestingly, the relative ion intensities and isotope-like patterns in their product ion spectra depend on the functional groups and ion forms of sugar chains. Consequently, the results indicate that a proton ( $\text{H}^+$ ) localizes on the amino group of the amino sugar, and that the proton ( $\text{H}^+$ ) induces their fragmentation.

Sodium cation ( $\text{Na}^+$ ) attachment is independent from amino group and exerts no influence on their fragmentation patterns in amino group except for mono- and disaccharide fragment ions because there is the possibility of the reducing end effect. In contrast, a sodium cation localizes much more frequently on the acetamide group in acetamide-CyDs because the chemical species with HexNAC are stable. Thus, their ions with HexNAC are abundant. These results are consistent with the fragmentation of lacto-neo-*N*-tetraose and maltotetraose, suggesting that a sodium cation generally localizes much more frequently on the acetamide group in sugar chains.

**Key words:** Oligosaccharides, MS/MS, Fragmentation, Sugar chains

Received: 4 May 2013/Revised: 31 July 2013/Accepted: 7 August 2013/Published online: 24 October 2013

## Introduction

Oligosaccharide structures have been analyzed by mass spectrometry (MS) and MS/MS techniques. Matrix-assisted laser desorption/ionization (MALDI) MS [1] and electrospray ionization (ESI) MS [2] are routinely used for sugar chain analyses. Large and complex sugar chain structures can be elucidated based on MS/MS analyses using methods such as time-of-flight tandem (TOF/TOF) MS [3], ion-trap TOF [4–8], and quadrupole TOF hybrid MS [9]. The fragmentation of sugar chains from positively charged molecules takes place at glycosyl bonds predominantly in low energy collision-induced dissociation (CID) [10] and in post-source decay (PSD) [11] or laser induced dissociation in MALDI-MS. Cross-ring fragments are

promoted in high-energy CID [3, 10]. Relative ion abundance analysis of the fragment ions is a very powerful strategy to distinguish the structures of isomeric sugar chains [3–16], and structural identification may also be achieved by MS/MS spectral pattern matching based on the relative ion abundance analysis of the fragment ions produced by glycosyl bond cleavages [4–8, 13–15]. MS/MS spectral patterns depend on many factors such as the sugar chain structure, sugar content, ionic forms of sugars, ionization methods, etc. Recently, computer simulations of sugar chain fragmentation in the gas phase [17, 18] have been used to predict the product ion spectra from MS/MS experiments [3–16]. The charge location is an important factor in calculating stable conformations and predicting fragmentation patterns. Neutral sugar chains have no charge-center, thus, their ionizations in MALDI and ESI are achieved by proton or alkali metal cation attachment. Until now, amino/acetamide sugar effects on ionization and fragmentation have not been studied experimentally. We focus our attention on differences among the hydroxy group of glucose (Glc), the amino group of hexosamine (HexNH<sub>2</sub>), and the acetamide group of *N*-acetyl hexosamine (HexNAC) in ionization and fragmentation. The sugar chains

**Electronic supplementary material** The online version of this article (doi:10.1007/s13361-013-0739-1) contains supplementary material, which is available to authorized users.

Correspondence to: Tohru Yamagaki; e-mail: yamagaki@sunbor.or.jp

with biological activities are included in glycoproteins and proteoglycans; however, these sugar chains have complex branching structures. Their product ion MS/MS spectra are too complex to extract and analyze the amino/acetamide sugar effect on their MS and MS/MS product ion spectra. To reveal the effects of amino and acetamide groups, we chose the ideal analytes in which one sugar unit with amino or acetamide groups differs in long homo-oligosaccharides. Cyclo-malto-hexaose, heptaose, octaose, ( $\alpha$ -,  $\beta$ -,  $\gamma$ -cyclodextrins; CyDs) are composed of six to eight  $\alpha$ -D-glucopyranoses linked by  $\alpha$ 1-4 glycosyl bond, which are cyclic homo gluco-oligosaccharides without reducing and non-reducing ends. So, if one residue of HexNH<sub>2</sub> or HexNAc is inserted in these compounds, the position of the hetero-sugar residue in the homo-oligosaccharides can be identified to only one structure as shown Figure 1. 3A-Amino-3A-deoxy-(2AS,3AS)-Cyclodextrins are Amino-CyDs (NH<sub>2</sub>-CyDs). 3A-acetamide-3A-deoxy-cyclodextrins are acetamide-CyDs (NAc-CyDs) prepared from amino-CyDs chemically. The reducing and non-reducing end effects can be neglected for ionization and fragmentation to them. These compounds are analyzed by MALDI TOF/TOF and ESI Q-TOF mass spectrometry and those results are

compared with that of conventional CyDs. Using this analytical system, it is possible to focus on the influence of the amino/acetamide sugar residues on fragmentation because the structural differences among CyDs, amino-CyDs, and acetamide-CyDs are attributable to just an amino or acetamide sugar residue.

## Experimental Methods

### Materials

$\alpha$ -,  $\beta$ -,  $\gamma$ -CyD were provided by Ensuiko Sugar Refining Co. Ltd., Yokohama, Japan. 3A-amino-3A-deoxy-(2AS,3AS)-cyclodextrins (Figure 1) were purchased from Tokyo Chemical Industry Co. Ltd., Tokyo, Japan. Maltotetraose was purchased from Hayashibara Biochemical Laboratories, Inc., Okayama, Japan. Lacto-neo-*N*-tetraose (LnNT) was purchased from Funakoshi, Co., Tokyo, Japan. 2,5-Dihydroxybenzoic acid (DHB) and  $\alpha$ -cyano-4-hydroxy cinnamic acid (CHCA) (Sigma-Aldrich, St. Louis, MO, USA) used as matrix were ultrapure reagent grade. 3A-acetamide-3A-deoxy-(2AS,3AS)-cyclodextrins (Figure 1) were prepared from amino-CyDs treated with acetic anhydride in sodium hydrogen

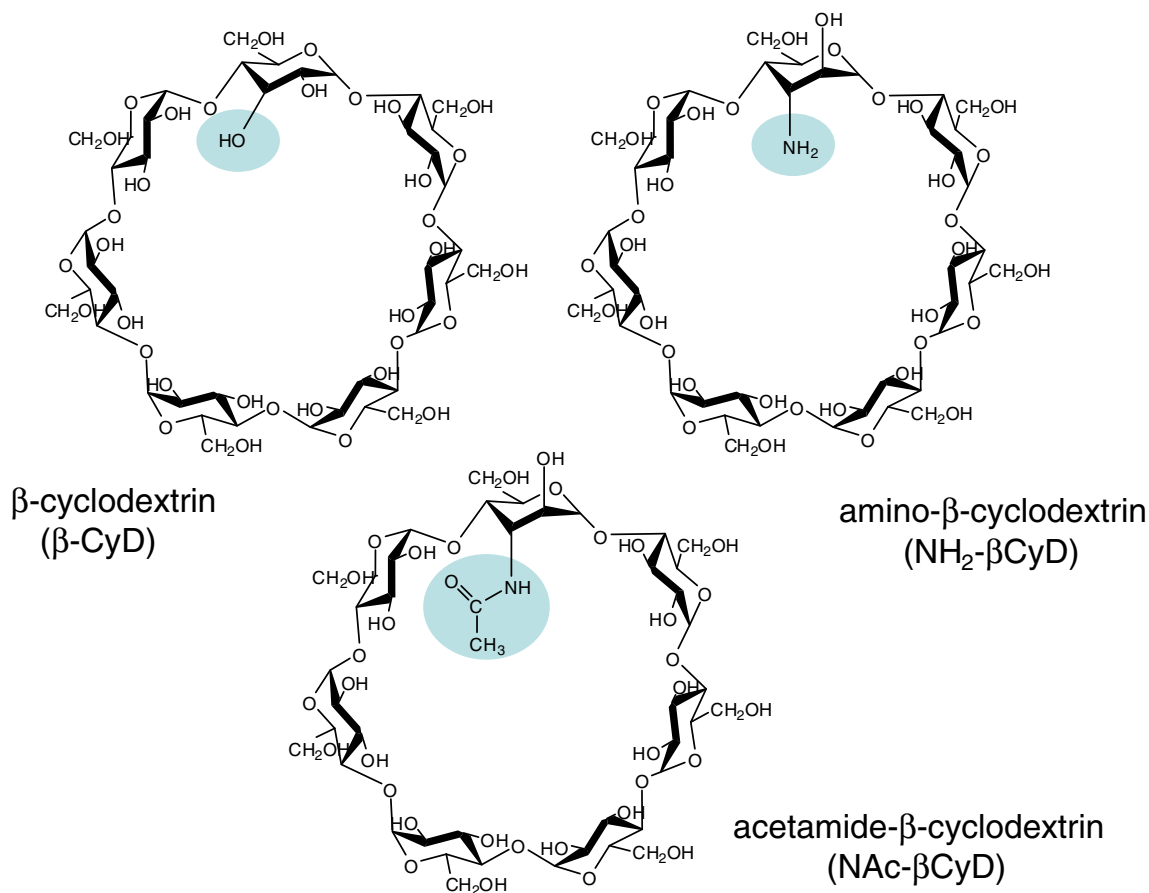


**Figure 1.** Structure of  $\beta$ -cyclodextrin ( $\beta$ -CyD), 3-amino-3-deoxy-(2AS,3AS)- $\beta$ -cyclodextrin (amino- $\beta$ CyD) and 3-acetamide-3-deoxy-(2AS,3AS)- $\beta$ -cyclodextrin (acetamide- $\beta$ CyD)

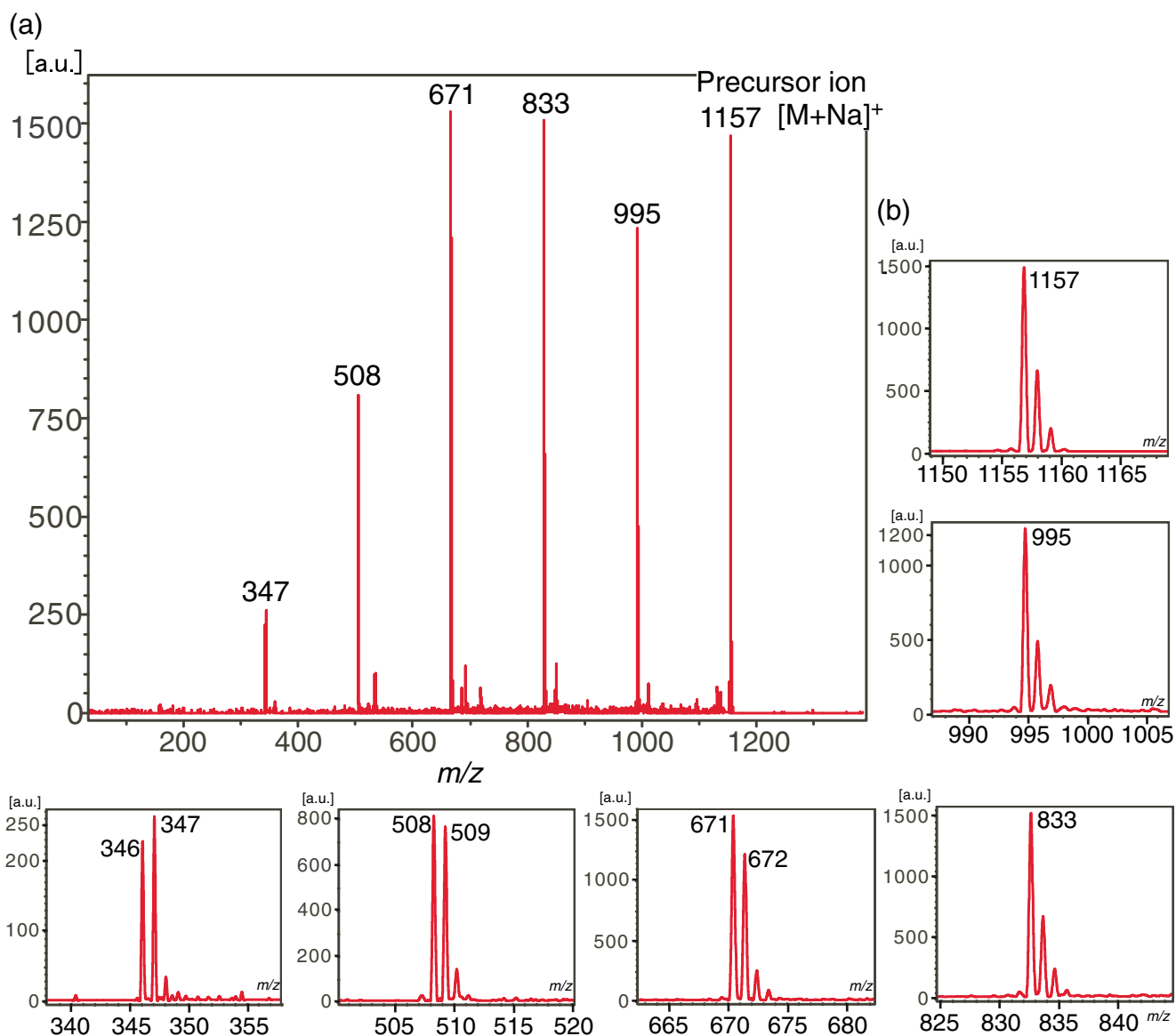


**Figure 2.** The LID product ion spectrum **(a)** of amino- $\beta$ CyD from the sodium cationized molecule, and the expanded spectra **(b)** in MALDI TOF/TOF mass spectrometry

carbonate aqueous solution on ice. The products were passed through a Dowex 50WX8 ion exchange column (Sigma-Aldrich), and were treated with sodium hydroxide in methanol to remove acetyl moieties on hydroxy groups.

### Mass Spectrometry

MALDI TOF mass and tandem TOF mass spectra were acquired on an Ultraflex III<sub>TOF/TOF</sub> MALDI TOF/TOF instrument (Bruker Daltonics GmbH, Bremen, Germany). The precursor ion for measuring laser induced dissociation (LID) spectra was set at  $\pm 5$  Da window range. All

analytes of CyD, amino-CyD, and acetamide-CyDs were prepared at 1 mg/mL concentration in aqueous solution. DHB was dissolved in 50 % ethanol aqueous solution at 10 mg/mL concentration. CHCA was in 80 % acetonitrile aqueous solution with 0.1 % formic acid at 10 mg/mL concentration.

Electrospray ionization MS (ESI-MS) and collision-induced dissociation (CID) MS/MS product ion spectra were acquired on a quadrupole time-of-flight (Q-TOF) hybrid mass spectrometry instrument (Q-ToF Micromass Waters, Co., Manchester, UK). Samples were dissolved in methanol-water (50:50, vol/vol) or in 100 mM ammonium acetate buffer at a final concentration of 5  $\mu$ M.

**Table 1.** Estimated Product Ions and Chemical Species Ratios of Amino- $\beta$ CyD

Precursor Ion	Na <sup>+</sup> /H <sup>+</sup> form m/z	Sugar res. (n)	(Glc <sub>n-1</sub> HexNH <sub>2</sub> )	Glc <sub>n</sub>
Precursor Ion	(m/z 1156/1134)	7		
[M - Sugar <sub>1</sub> ] <sup>+</sup>	(m/z 994/972)	6	6 :	1
[M - Sugar <sub>2</sub> ] <sup>+</sup>	(m/z 832/810)	5	5 :	2
[M - Sugar <sub>3</sub> ] <sup>+</sup>	(m/z 670/648)	4	4 :	3
[M - Sugar <sub>4</sub> ] <sup>+</sup>	(m/z 508/486)	3	3 :	4
[M - Sugar <sub>5</sub> ] <sup>+</sup>	(m/z 347/324)	2	2 :	5
[M - Sugar <sub>6</sub> ] <sup>+</sup>	(m/z 185/162)	1	1 :	6

\*Sugar includes Glc and HexNH<sub>2</sub>.

The chemical species of the amino- $\beta$ CyD product ions are estimated assuming random cleavage of the glycosyl bonds

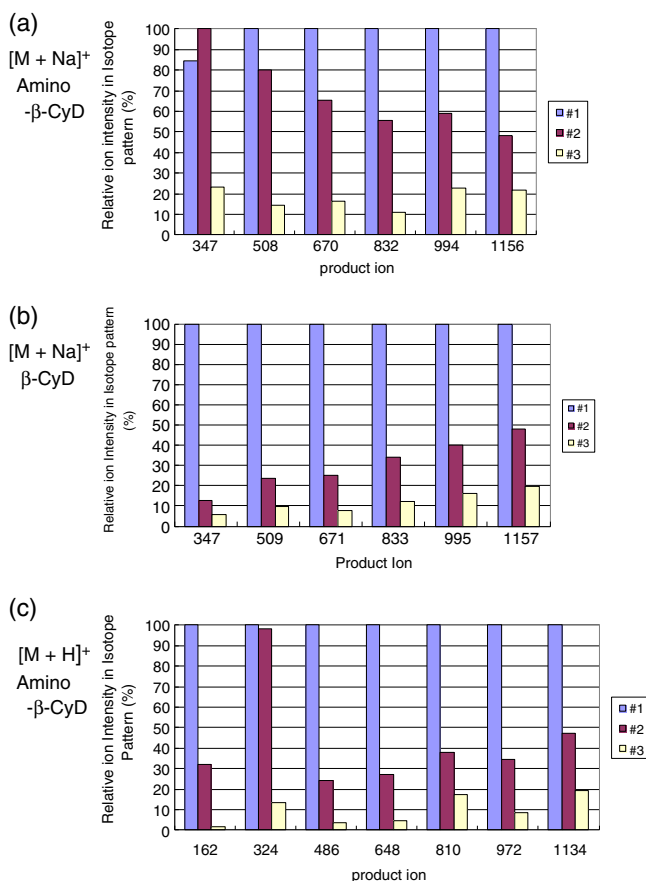
## Results and Discussion

In the MALDI-TOF MS, the sodium cationized molecules [M + Na]<sup>+</sup> are observed in the spectra from all of conventional CyDs, amino-CyDs, and acetamide-CyDs (summarized in Supporting Information-1). The protonated molecules [M + H]<sup>+</sup> are generated only from amino-CyDs using DHB (Supporting information-2). In the case of CHCA with 0.1 %–1.0 % formic acid, there are no peaks of the protonated molecules of all CyDs, amino-CyD (very small), and acetamide-CyDs in the spectra even though CHCA is a well-known matrix for peptides as the protonated molecules. Therefore, all MALDI-MS data are acquired with DHB as a proper matrix in this study.

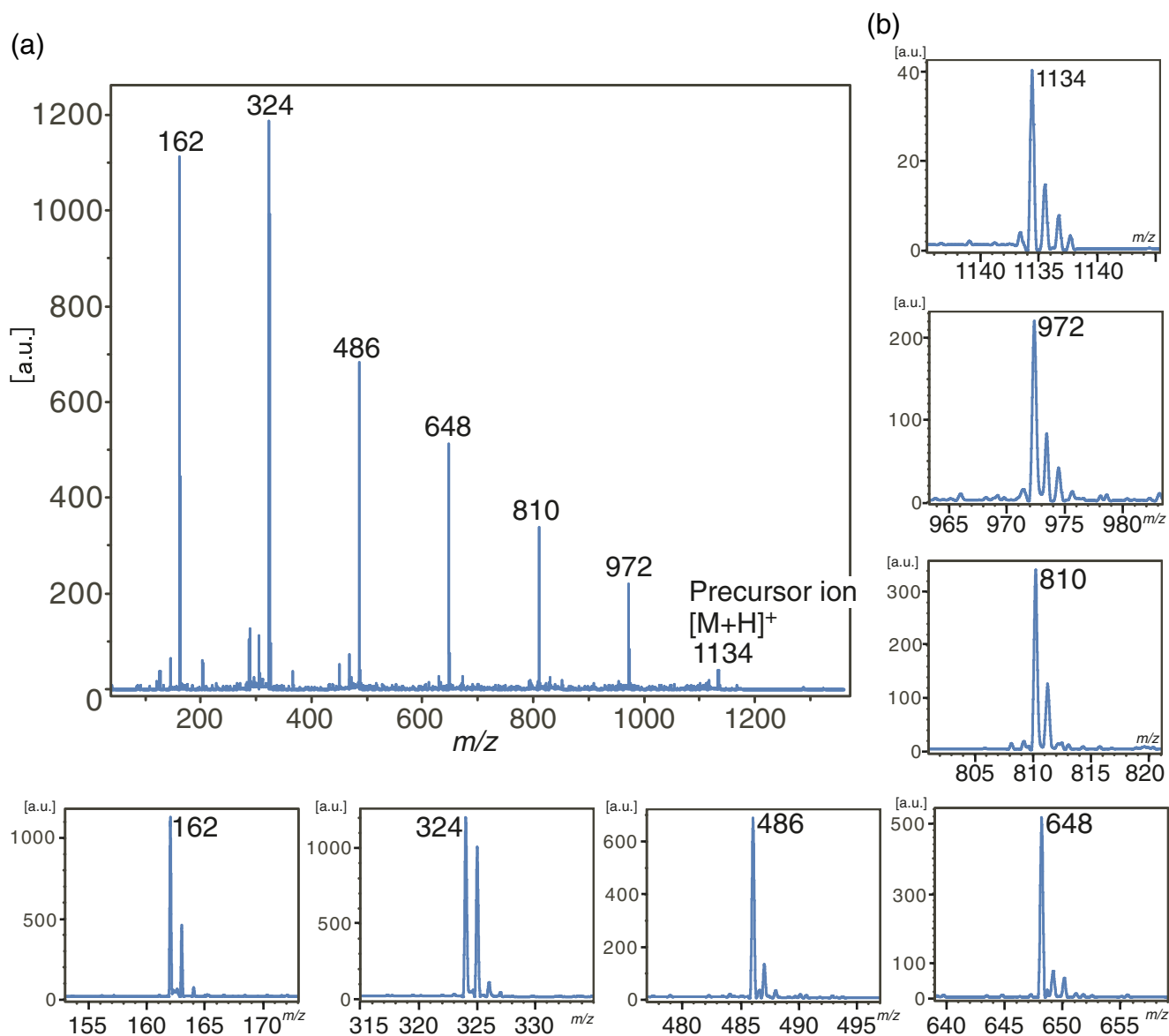
To study the affinities of sodium cation for amino group, the ionization efficiency among  $\beta$ CyD, amino- $\beta$ CyD, and acetamide- $\beta$ CyD are estimated by comparing each peak intensity with that of the internal standard of  $\alpha$ -CyD. The ionization efficiency of  $\beta$ CyD and amino- $\beta$ CyD is almost the same extent; in contrast, that of acetamide- $\beta$ CyD is higher than  $\beta$ CyD and amino- $\beta$ CyD (Supporting Information-3). The results indicate that the amino group does not influence the sodium cation affinity and that the acetamide group has high affinity to sodium cation. This finding suggests that sodium cation frequently localizes at acetamide group rather than amino and hydroxy groups (Supporting Information-3). In the ESI-MS spectra of  $\beta$ -CyD, amino- $\beta$ CyD, and acetamide- $\beta$ CyD, both the protonated molecule [M + H]<sup>+</sup> and the sodium cationized molecule [M + Na]<sup>+</sup> are detected (Supporting Information-1).

Figure 2 shows the LID product ion spectra of amino- $\beta$ CyD from the sodium cationized molecule [M + Na]<sup>+</sup> at *m/z* 1156.9 using MALDI-TOF/TOF MS. The product ions of amino- $\beta$ CyD are produced by the loss of hexose units (Table 1), and cleavages of two glycosidic bonds are required (Supporting information-4) [11]. Comparing the isotope-like patterns of the product ions, the second peak intensity from the left elevates as the sugar units decreased (Figure 2). This is because the chemical species of the amino- $\beta$ CyD product ions do not unify (Table 1); they are

mixtures of two distinct chemical species with or without an amino sugar residue (HexNH<sub>2</sub>). The shifting ratio of these chemical species cause abnormal isotope-like peak patterns of the product ions. Table 1 shows the calculated ratios of the chemical species for each product ion when sodium cation attaches to any sugar residues, in which the glycosyl bonds then decompose randomly. The components of these chemical species reversed at the signals between *m/z* 670 and 508 (Table 1). There is an obvious change in the isotope-like peak pattern at *m/z* 670 in the LID spectra (Figure 2). In the ESI-MS and MS/MS (Figure 3), the product ions from the sodium cationized molecule shows the same tendency. In Figure 3, the ion intensity of each product ion is normalized to the highest isotope-like peak to estimate the variation of the relative intensities. The relative intensities of the second isotope ions of amino- $\beta$ CyD are elevated



**Figure 3.** ESI CID-MS/MS isotopic-like peak pattern of the product ions (a) from the sodium cationized molecule [M + Na]<sup>+</sup> of amino- $\beta$ CyD, (b) the conventional CyD, and (c) from the protonated molecule [M + H]<sup>+</sup> of amino- $\beta$ CyD in ESI Q-TOF mass spectrometry. Three isotope signals of each product ion make a set, and the relative ion intensities were normalized to the highest signal (100 %) among the three isotope signals



**Figure 4.** The LID product ion spectrum **(a)** of amino- $\beta$ CyD from the protonated molecule  $[M + H]^+$ , and the expanded spectra **(b)** in MALDI TOF/TOF mass spectrometry

in the smaller product ions in the ESI-MS/MS product ion spectrum from the sodium cationized molecule  $[M + Na]^+$  of amino- $\beta$ CyD (Figure 3a). These results suggest that sodium cation cannot localize at only HexNH<sub>2</sub> residues in amino- $\beta$ CyD and that the glycosyl bonds are also cleaved randomly in amino- $\beta$ CyD  $[M + Na]^+$ . The amino group effects can be almost neglected in the long sugar chain species over trioses, but the intensity pattern of the biose of the product ion at  $m/z$  346 is not consistent with the ratio of the calculated chemical species (Table 1 and Figures 2 and 3). There is one of the possibilities that the reducing end in the small chemical species of biose at least causes those results.

In contrast, the second isotope peaks of the product ions decrease as the product ion masses decrease (Figure 4) in MALDI LID product ion spectrum of amino- $\beta$ CyD, indicating that the chemical species of the product ions of amino- $\beta$ CyDs include an amino sugar residue (Table 1). This further indicates that the protonation site is fixed at the amino sugar and that the chemical species of the product ions are unified because the charge center is fixed at the amino group. In fact, the protonated HexNH<sub>2</sub> residue signal at  $m/z$  162 is predominantly detected and the glucose peak at  $m/z$  163 is barely detectable (Figure 4), even though the number of HexNH<sub>2</sub> is one-sixth that of Glc residues in amino- $\beta$ CyD (Table 1).

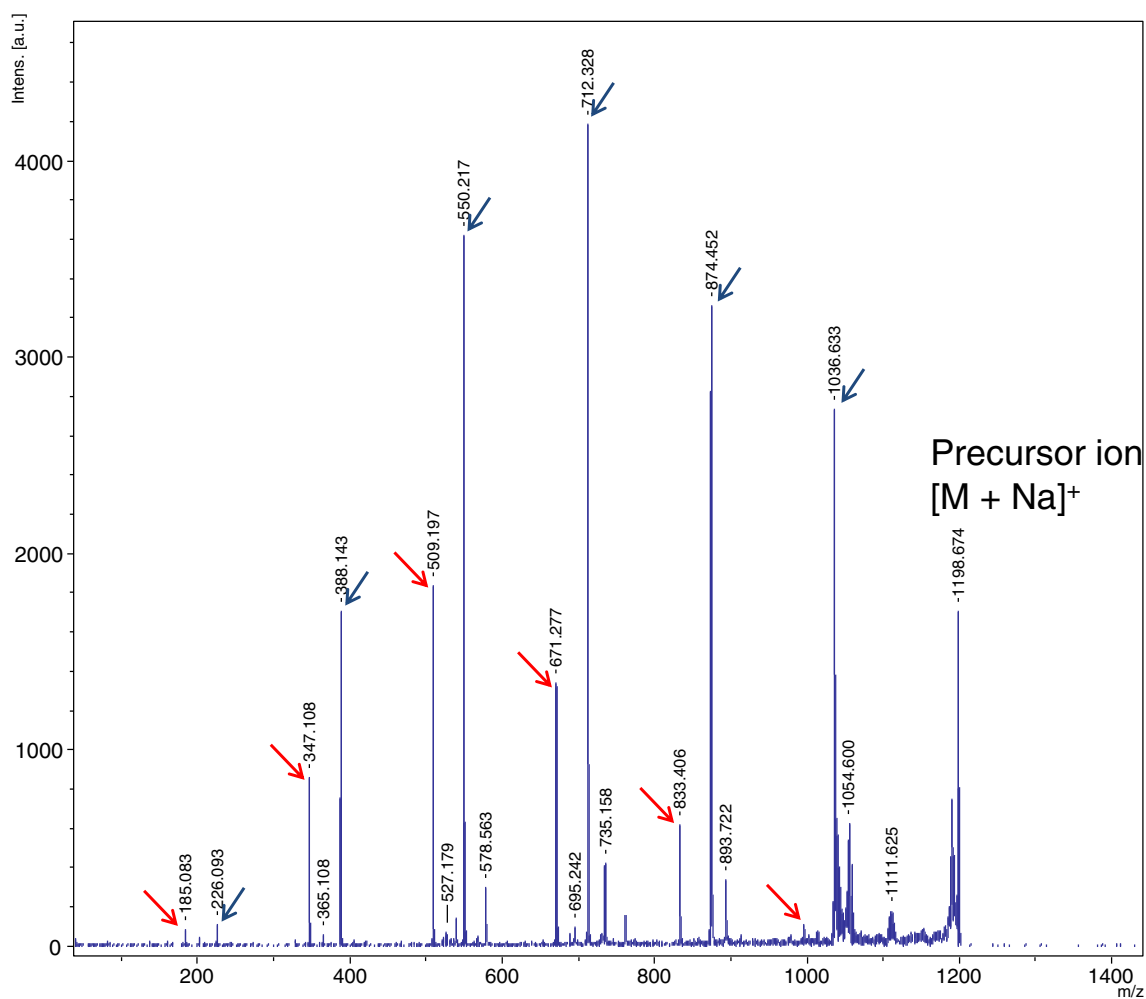


**Figure 5.** The LID product ion spectrum from the sodium cationized molecule  $[M + H]^+$  of acetamide- $\beta$ CyD by MALDI TOF/TOF Mass spectrometry. The peaks labeled by blue and red arrows originated from the chemical species with or without HexNAc, respectively

The isotope-like ion patterns of the product ions between amino- $\beta$ CyD and conventional CyD are almost the same in the ESI CID-MS/MS product spectra from their protonated molecules  $[M + H]^+$  (Figure 3b and c). It indicates that amino sugar HexNH<sub>2</sub> unit is preserved in the chemical species of the product ions of amino- $\beta$ CyD, although the disaccharide product ion is excepted because the HexNH<sub>2</sub> is partially removed in the chemical species. Consequently, these results of ESI CID-MS/MS are consistent with those of MALDI LID product ion spectra. This tendency in the relative ion intensities is independent from the collision energies of the ESI CID and the irradiation laser power of MALDI LID.

With regard to the relative intensity of the product ions, the lower mass ions have higher intensities than the higher mass ions in the MALDI LID spectrum (Figure 4) and in the ESI CID MS/MS spectrum (Figure 3c) from the protonated amino- $\beta$ CyD molecule  $[M + H]^+$ . This tendency of the spectral patterns is different from that of

the sodium cationized molecule  $[M + Na]^+$ . The small product ions are not generated from the multi-decompositions of the large ions. The glycoside bonds close to the protonated HexNH<sub>2</sub> residue are likely to decompose

**Table 2.** Estimated Product Ions Chemical Species Ratio of Acetamide- $\beta$ CyD

	Sugar res. ( <i>n</i> )	(Glc <sub><i>n-1</i></sub> HexNH <sub>2</sub> )	Glc <sub><i>n</i></sub>
Precursor ion ( <i>m/z</i> 1198)	7		
* $[M - \text{Sugar}_1 + Na]^+$	6	6 ( <i>m/z</i> 1036)	1 ( <i>m/z</i> 1036)
$[M - \text{Sugar}_2 + Na]^+$	5	5 ( <i>m/z</i> 874)	2 ( <i>m/z</i> 833)
$[M - \text{Sugar}_3 + Na]^+$	4	4 ( <i>m/z</i> 712)	3 ( <i>m/z</i> 671)
$[M - \text{Sugar}_4 + Na]^+$	3	3 ( <i>m/z</i> 550)	4 ( <i>m/z</i> 509)
$[M - \text{Sugar}_5 + Na]^+$	2	2 ( <i>m/z</i> 388)	5 ( <i>m/z</i> 374)
$[M - \text{Sugar}_6 + Na]^+$	1	1 ( <i>m/z</i> 226)	6 ( <i>m/z</i> 185)

\* Sugar includes Glc and HexNAc.

The chemical species of the amino- $\beta$ CyD product ions were estimated assuming random cleavage of the glycosyl bonds



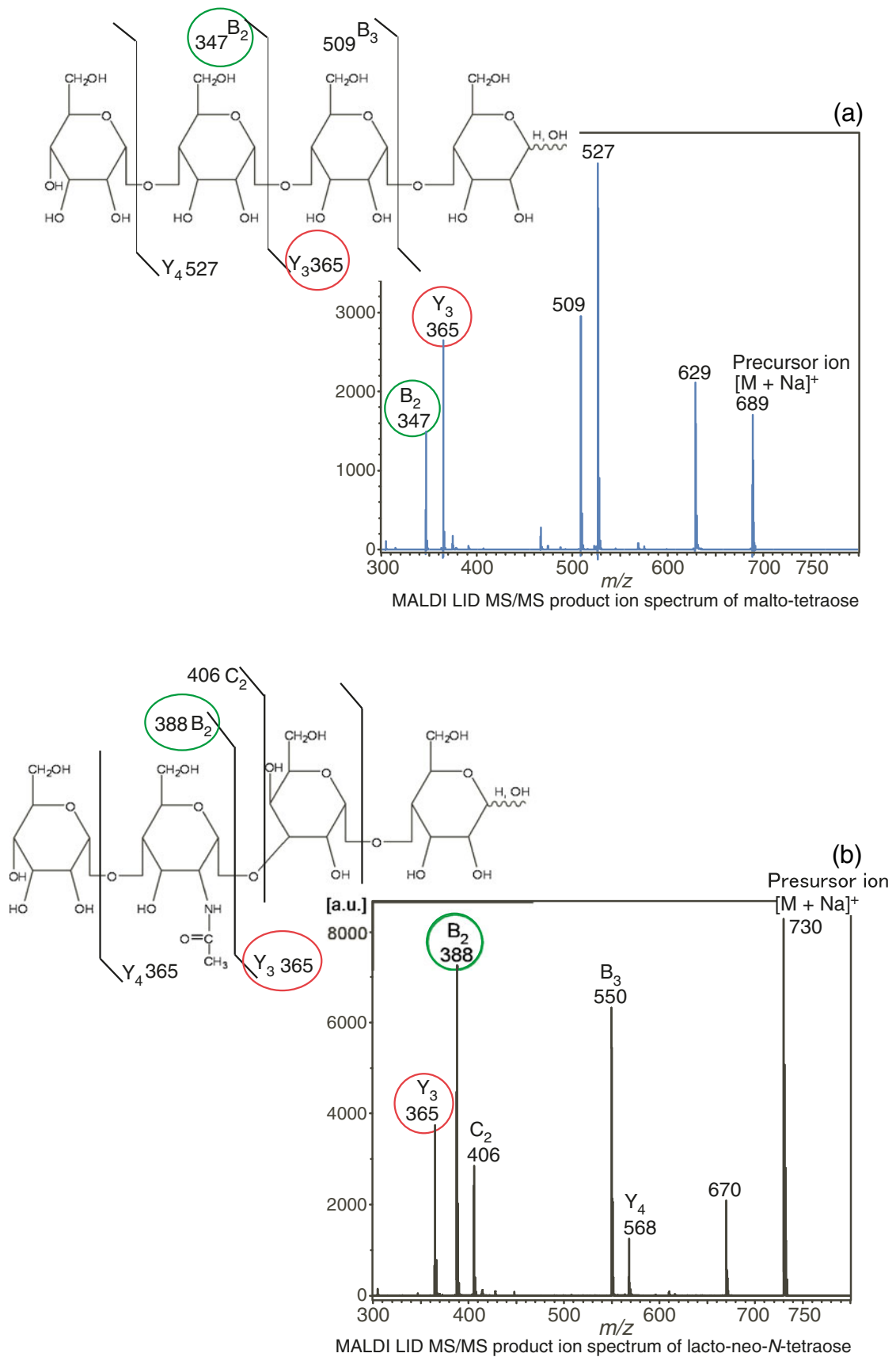


**Figure 6.** Comparison of **(a)** maltotetraose and **(b)** lacto-neo-*N*-tetraose (LnNT) spectra and their fragmentation patterns

in the protonated molecules easily, and the small product ions are generated abundantly. The proton on the protonated molecules is directly involved in the fragmentation process and the mobile proton promotes the fragmentation around the easily proton-associated HexNH<sub>2</sub> residue.

The ESI CID reaction curves are plotted as a function of the collision energy in the ESI Q-TOF MS (Supporting Information-5). The cross point for the abundance of precursor and product ions from the protonated molecule is apparently lower than that of the sodium cationized molecule in amino-βCyD. The sodium cationized molecules of amino-βCyD and β-CyD require almost the same collision energy for their CIDs. These results indicate that the protonated molecules decompose more easily than the sodium cationized molecules and that the decomposition from the protonated molecule depends on the amino group, whereas that from the sodium cationized molecule is independent of the amino group.

Figure 5 shows the MALDI LID product ion spectrum of acetamide-βCyD from the sodium cationized molecule [M + Na]<sup>+</sup>. There are two separated series of the peaks with or without *N*-acetyl hexosamine. These product ions can be assigned and summarized in Table 2 because the molecular masses between Glc and HexNAc are 41 Da. The ion peaks labeled with blue arrows are assigned to the species with HexNAc as Glc<sub>n-1</sub>HexNAc and the ion peaks labeled with red arrows are assigned to the species without HexNAc as Glc<sub>n</sub> in Table 2 and Figure 5. The ion intensity of the product ion with HexNAc is much higher than those without HexNAc, indicating that sodium cations localize on the acetamide hexose residue (HexNAc) frequently.

The MALDI LID product ion spectra of tetrasaccharides with or without *N*-acetyl glucosamine residue (GlcNAc) are compared to generally prove the acetamide group effects on the ionization and fragmentation of linear sugar chains. Figure 6 shows the MALDI-LID product ion spectra of maltotetraose and lacto-neo-*N*-tetraose (LnNT). The Y type product ions with a reducing terminal have a higher intensity than the B type ions in the spectrum of a homogeneous glucotetraose of maltotetraose. The product ion Y<sub>3</sub> of maltotetraose is more intense than the ion B<sub>2</sub>. In contrast, the product ions including GlcNAc of LnNT have higher intensity than the others [16]. This result indicates that GlcNAc has a higher affinity for sodium cation and that it thus can be the charge center.

## Conclusions

Amino and acetamide groups influence the fragmentation of sugar chains and their effects depend on the specific ion forms. In sugar chains with amino sugar (HexNH<sub>2</sub>), the sodium cations can coordinate to any sugars and glycosyl bonds are likely to cleave randomly. In contrast,

the influence on the fragmentation from protonated molecules including the amino sugar is substantial. Protons localize at the amino group in sugar chains, and the product ions include the protonated amino sugar. The mobile protons can induce glycosyl bond cleavage, and fragmentation frequently takes place close to the amino sugar residues. In the case of an acetamide sugar (HexNAc), the sodium cation locates on the acetamide group, and the product ions, including HexNAc, predominate in the MS/MS spectra. These findings are reproducible in both MALDI-LID and ESI hexapole CID. These fragmentation tendencies will likely prove to be useful for the prediction of MS/MS fragmentation patterns of sugar chains by computer simulations.

## Acknowledgments

The authors thank Dr. Hajime Komura (Suntory Institute for Bioorganic Research) for his technical supports of chemical synthesis, and Ms. Akiko Segawa (Suntory Institute for Bioorganic Research) for her support of MS and HPLC measurements.

## Open Access

This article is distributed under the terms of the Creative Commons Attribution License which permits any use, distribution, and reproduction in any medium, provided the original author(s) and the source are credited.

## References

1. Harvey, D.J.: Analysis of carbohydrates and glycoconjugates by matrix-assisted laser desorption/ionization mass spectrometry: an update covering the period 1999–2000. *Mass Spectrom. Rev.* **25**, 595–662 (2006)
2. Wacker, M., Linton, D., Hitchen, P.G., Nita-Lazar, M., Haslam, S.M., North, S.J., Panico, M., Morris, H.R., Dell, A., Wren, B.W., Aebi, M.: *N*-Linked glycosylation in *Campylobacter jejuni* and its functional transfer into *E. coli*. *Science* **298**, 1790–1793 (2002)
3. Mechref, Y., Novotny, M.V.: Structural characterization of oligosaccharides using MALDI-TOF/TOF tandem mass spectrometry. *Anal. Chem.* **75**, 4895–4903 (2003)
4. Takegawa, Y., Ito, S., Yoshioka, S., Deguchi, K., Nakagawa, H., Monde, K., Nishimura, S.: Structural assignment of isomeric 2-aminopyridine-derivatized oligosaccharides using MS<sup>n</sup> spectral matching. *Rapid Commun. Mass Spectrom.* **18**, 385–391 (2004)
5. Takegawa, Y., Seguchi, K., Ito, S., Yoshioka, S., Nakagawa, H., Nishimura, S.: Simultaneous analysis of 2-aminopyridine-derivatized neutral and sialylated oligosaccharides from human serum in the negative-ion mode by sonic spray ionization ion trap mass spectrometry. *Anal. Chem.* **77**, 2097–2106 (2005)
6. Ito, H., Takegawa, Y., Deguchi, K., Nagai, S., Nakagawa, H., Shinohara, Y., Nishimura, S.: Direct structural assignment of neutral and sialylated *N*-glycans of glycopeptides using collision-induced dissociation MS<sup>n</sup> spectral matching. *Rapid Commun. Mass Spectrom.* **20**, 3557–3565 (2006)
7. Kameyama, A., Kikuchi, N., Nakaya, S., Ito, H., Sato, T., Sshikanai, T., Takahashi, Y., Takahashi, K., Narimatsu, H.: A strategy for identification of oligosaccharide structures using observational multistage mass spectral library. *Anal. Chem.* **77**, 4719–4725 (2005)
8. Kameyama, A., Nakaya, S., Ito, H., Kikuchi, N., Angata, T., Nakamura, M., Ishida, H., Narimatsu, H.: Strategy for simulation of CID spectra of *N*-linked oligosaccharides toward glycomics. *J. Proteome Res.* **5**, 808–814 (2006)



9. Harvey, D.J.: Fragmentation of negative ions from carbohydrates. Part 1. Use of nitrate and other anionic adducts for the production of negative ion electrospray spectra from *N*-linked carbohydrates. *J. Am. Soc. Mass Spectrom.* **16**, 622–630 (2005)
10. Reinhold, V.N., Reinhold, B.B., Costello, C.E.: Carbohydrate molecular weight profiling, sequence, linkage, and branching data: ES-MS and CID. *Anal. Chem.* **67**, 1772–1784 (1995)
11. Yamagaki, T., Ishizuka, Y., Kawabata, S., Nakanishi, H.: Postsource decay fragment spectra of cyclomalto-octaose and branched cyclomaltohexaose by matrix-assisted laser desorption/ionization time-of-flight mass spectrometry. *Rapid Commun. Mass Spectrom.* **10**, 1887–1890 (1996)
12. Yamagaki, T., Nakanishi, H.: Ion intensity analysis of post-source decay fragmentation in curved-field reflectron matrix-assisted laser desorption/ionization time-of-flight mass spectrometry of carbohydrates: For structural characterization of glycosylation in proteome analysis. *Proteomics* **1**, 329–339 (2001)
13. Everest-Dass, A.V., Kolarich, D., Campbell, M.P., Packer, N.H.: Tandem mass spectra of glycan substructures enable the multistage mass spectrometric identification of determinants on oligosaccharides. *Rapid Commun. Mass Spectrom.* **27**, 931–939 (2013)
14. Wu, S., Tao, N., German, J.B., Grimm, R., Lebrilla, C.B.: Development of an annotated library of neutral human milk oligosaccharides. *J. Proteome Res.* **9**, 4138–4151 (2010)
15. Wu, S., Salcedo, J., Tang, N., Waddell, K., Grimm, R., German, J.B., Lebrilla, C.B.: Employment of tandem mass spectrometry for the accurate and specific identification of oligosaccharide structures. *Anal. Chem.* **84**, 7456–7462 (2012)
16. Yamagaki, T., Nakanishi, H.: Distinguishing of linkage isomers of lactotetra oligosaccharides by using the relative ion intensity analysis of post-source decay fragment ions in curved-field reflectron matrix-assisted laser desorption/ionization time-of-flight mass spectrometry. *Anal. Sci.* **17**, 83–87 (2001)
17. Mizuno, Y., Sasagawa, T., Dohmae, N., Takio, K.: An automated interpretation of MALDI/TOF postsource decay spectra of oligosaccharides. 1. Automated peak assignment. *Anal. Chem.* **71**, 4764–4771 (1999)
18. Ethier, M., Saba, J.A., Spearman, M., Krokhin, O., Butler, M., Ens, W., Standing, K.G., Perreault, H.: Application of the StrOligo algorithm for the automated structure assignment of complex *N*-linked glycans from glycoproteins using tandem mass spectrometry. *Rapid Commun. Mass Spectrom.* **17**, 2713–2720 (2003)